## Article Information

**Journal Title:** Journal of guidance, control, and dynamics

**Volume:** 9 **Issue:** 3
**Month/Year:** 1986-05**Pages:** 294-303

**Article Author:** JUANG, J.-N.

**Article Title:** Effects of noise on modal parameters identified by the Eigensystem Realization Algorithm

## Loan Information

**Loan Title:**

**Loan Author:**

**Publisher:**
**Place:**
**Date:**
**Imprint:**

## Customer Information

**Username:** hpgavin@duke.edu

Henri Gavin
771822661
Faculty - Engineering

Article Delivery Method: Hold for Pickup
Loan Delivery Method: Hold for Pickup
Electronic Delivery? Yes

# Effects of Noise on Modal Parameters Identified by the Eigensystem Realization Algorithm

Jer-Nan Juang* and Richard S. Pappa†
*NASA Langley Research Center, Hampton, Virginia*

**The basic concept of the Eigensystem Realization Algorithm for modal parameter identification and model reduction is extended to minimize the distortion of the identified parameters caused by noise. The mathematical foundation for the properties of accuracy indicators, such as the singular values of the data matrix and modal amplitude coherence, is provided, based on knowledge of the noise characteristics. These indicators quantitatively discriminate noise from system information and are used to reduce the realized system model to a better approximation of the true model. Monte Carlo simulations are included to support the analytical studies.**

## Introduction

SYSTEM identification using dynamic tests has been extensively incorporated into the design development, quality control, and qualification of dynamic systems. Dynamic tests typically involve applying a forcing excitation on the system and measuring the response at various locations. The dynamic behavior identified from the tests can then be used for validating or improving the design. The accuracy of theoretical predictions of behavior can also be checked.

The knowledge of system behavior is generally called a model. The model may be given in any one of several different forms, such as transfer functions, differential equations, or modal parameters. Also, many different methods are available for identifying the parameters of the model.[1,2] For example, in a real-time controller design the dynamic behavior may be determined by reflection coefficients[3] in a linear regression model. The reflection coefficients can be updated on-line at each time instant when new data become available. The simple and special mathematical structure of the linear regression model makes the identification possible in real time. For identification of structures, on the other hand, the dynamic behavior is usually represented by the modal parameters (natural frequencies, modal damping, mode shapes, and generalized mass).[4] Modal parameters provide physical intuition and interpretation of the system characteristics and are the usual link in the structures field for comparison with theoretical predictions.

The basic development of the time-domain (state-space) concept is attributed to Ho and Kalman,[5] who introduced the important principles of minimal realization theory. The Ho-Kalman procedure uses a sequence of real matrices known as Markov parameters (impulse response functions) to construct a state-space representation of a linear system. Among follow-up developments along similar lines on minimal realization theory, an Eigensystem Realization Algorithm (ERA) for modal parameter identification and system model reduction was developed.[6] The method has been successfully applied to several sets of structural dynamics data, such as from the Galileo spacecraft modal survey[7] and the Solar Array Flight Experiment.[8]

The objective of this paper is to study the influence of noise on modal parameters identified by the ERA. As part of that algorithm, several accuracy indicators, such as the singular values of the block data matrix and a parameter referred to as Modal Amplitude Coherence, are used to evaluate the effects of noise on the identified parameters. Although these indicators were supported by good simulation and experimental results, they were ad hoc and heuristic in the sense that their quantitative relationship with the noise characteristics of the data was unknown. This paper establishes the mathematical foundation for the characteristics of the accuracy indicators based on noise information. Using these indicators, model reduction can be performed by retaining only those modal parameters with high accuracy indicators.

The paper is organized as follows. First, the basic formulation of the ERA is reviewed and extended to allow a more general arrangement of the data. The goal of this extension is to reduce the computational burden and the distortion of the identified parameters caused by noise. Next, the algebraic relationships between the noise characteristics and the accuracy indicators are established. Last, the validity of the analytical development is demonstrated, using results from Monte Carlo[9] numerical simulations.

## Basic Formulations

A finite-dimensional, discrete time, linear, time-invariant dynamic system can be represented by the state-variable equations

$$x(k+1)=Ax(k)+Bu(k), \quad B=[b_1, b_2, \ldots, b_m] \tag{1}$$

$$y(k)=Cx(k), \quad C^T=[c_1^T, c_2^T, \ldots c_p^T] \tag{2}$$

where $x$ is an $n$-dimensional state vector, $u$ is an $m$-directional input or control vector, and $y$ is a $p$-dimensional output or measurement vector. The integer $k$ is the sample indicator. The state transition matrix $A$ characterizes the dynamics of the system. For flexible structures, the matrix $A$ is a representation of mass, stiffness, and damping properties. The column vector $b_i$ is the control influence vector for the $i$th control input, and the row vector $c_j$ is the measurement influence vector for the $j$th measurement sensor.

Two special solutions to the state-variable Eqs. (1) and (2) are the impulse-response function (known as the Markov parameters)

$$y_{ji}(k)=c_jA^{k-1}b_i; \quad i=1,2,\ldots,m; \quad j=1,2,\ldots,p; \quad k=1,2,\ldots \tag{3}$$

and the initial-state-response function

$$y_{ji}(k)=c_jA^kx_i(0) \tag{4}$$

where $x_i(0)$ represents the $i$th set of initial conditions. The problem of minimal system realization is then the following:

Received Oct. 28, 1985; revision received Jan. 23, 1986. 

*Senior Research Scientist, Structural Dynamics Branch. Member AIAA.

†Research Engineer, Structural Dynamics Branch. Member AIAA.

Given the functions $y_{ji}(k)$, construct a set of constant matrices $[A, B, C]$ in terms of $y_{ji}(k)$ such that the identities of Eq. (3) hold and the order of $A$ is minimum.

Let the column index $I_0$ be the set of integers $(1,2,\ldots m)$, the column index $I_i\,(i=1,2,\ldots\eta)$ be any arbitrary subset of $I_0$, the row index $J_0$ be the set of integers $(1,2,\ldots,p)$, and the row index $J_j$ $(j=1,2,\ldots,\xi)$ be any arbitrary subset of $J_0$. The ERA begins by forming the $(\xi+1)$ by $(\eta+1)$ block data matrix

$$H(k-1)=[Y_{J_jI_i}(s_j+k+t_i)]; \quad i=1,2,\ldots,\eta \text{ and } j=1,2,\ldots,\xi \tag{5}$$

where $s_0=t_0=0$, $s_j$ and $t_i$ are arbitrary integers. and $Y$ is a rectangular matrix with entries the elements shown in Eq. (3) with appropriate indices $J_j$, $I_i$, $s_j$, $t_i$, and $k$. For example, when $i=j=0$

$$Y_{J_0I_0}(s_0+k+t_0) = \begin{bmatrix} y_{11}(k), & y_{12}(k), & \ldots & y_{1m}(k) \\ y_{21}(k), & y_{22}(k), & \ldots & y_{2m}(k) \\ & \vdots & & \\ y_{p1}(k), & y_{p2}(k), & \ldots & y_{pm}(k) \end{bmatrix} \tag{6}$$

Equation (5) is equivalent to deleting some rows and columns of the general Hankel matrix,[5,6] but maintaining the first block matrix [Eq. (6)] intact. Furthermore, using Eq. (5), the standard ordering of entries in the general Hankel does not need to be maintained.

In contrast to classical system realization methods which use a Hankel matrix,[5] the ERA block data matrix (Eq. 5) allows one to include only good or strongly measured signals without losing any capability. This is useful since some measurement data may be noisier than others or sensors may malfunction during the test. The advantage of this capability is the potential to minimize the distortion of the identified parameters caused by noise. A judicious choice of data and their proper arrangement in the block matrix $H(0)$ can also be used to minimize the computational requirements of the method. For example, the columns of $H(0)$ may be made as independent as possible by properly selecting the data samples to use as entries of the matrix. This effort could substantially reduce the order of the matrix for large problems. For noise-free data, the order can be the same as that of the system state matrix $A$. This fact results from examination of the controllability and observability matrices, to be discussed next.

From Eqs. (3-6), it can be shown that

$$H(k)=V_\xi A^k W_\eta; V_\xi = \begin{bmatrix} C \\ C_{J_1}A^{s_1} \\ \vdots \\ C_{J_\xi}A^{s_\xi} \end{bmatrix}$$
$$W_\eta = [B, A^{t_1}B_{I_1},\ldots,A^{t_\eta}B_{I_\eta}] \tag{7}$$

where $V_\xi$ and $W_\eta$ are generalized observability and controllability matrices. The columns of $B_{I_i}\,(i=1,2,\ldots,\eta)$ and the rows of $C_{J_j}\,(j=1,2,\ldots,\xi)$ are arbitrary subsets of $(b_1,b_2,\ldots,b_m)$ and $(c_1, c_2,\ldots,c_p)$, respectively. Note that both $W_\eta$ and $V_\xi^T$ have row number $n$, which is the order of the state matrix $A$, if the realized system $[A, B, C]$ is controllable and observable. For an $n$th-order system, only $n$ columns (not necessarily the first $n$) of $W_\eta$ and $V_\xi^T$ are needed theoretically to make the realization controllable and observable.

The realization problem involves the computation of the matrices $[A, B, C]$, as shown in Eqs. (1) and (2), from a given block matrix (Eq. 5). The basic concepts for noise-free data were developed long ago by Ho and Kalman.[5] The methodology has been recently extended for noisy measurement data for model parameter identification and model reduction of flexible structures.[6] A reliable implementation was developed.

The ERA process starts with the factorization of the block data matrix (Eq. 5), for $k=1$, using singular value decomposition:[10]

$$H(0)=P_N D_N Q_N^T \tag{8}$$

where the columns of $P_N$ and $Q_N$ are orthonormal and $D_N$ is diagonal

$$D_N=\text{diag}[d_1, d_2,\ldots,d_n, d_{n+1},\ldots,d_N] \tag{9}$$

with monotonically non-increasing $d_i\,(i=1,2,\ldots,N)$

$$d_1\geq d_2\geq\ldots\geq d_n\geq d_{n+1}\geq\ldots\geq d_N\geq 0 \tag{10}$$

This decomposition can be accomplished by readily available algorithms. Next, $D_N$ is replaced by a diagonal matrix $D_n$ that differs from $D_N$ only by the truncation of $d_{n+1},\ldots,d_N$. Correspondingly, $P_n$ and $Q_n$ are obtained by deleting the last $N-n$ columns of $P_N$ and $Q_N$, respectively. It will be shown in the next section of the paper that $P_nD_nQ_n^T$ is a matrix of rank $n$ which is closest to $H(0)$ in the sense of maximal signal-to-noise ratio.

Following the formulation in Ref. 6, a reduced-order realization of dimension $n$ can be constructed by forming

$$A^k=D_n^{-1/2}P_n^T H(k)Q_nD_n^{-1/2} \tag{11}$$

$$B=D_n^{1/2}Q_n^T E_{m1} \tag{12}$$

$$C=E_{p1}^T P_n D_n^{1/2} \tag{13}$$

where $E_{m1}^T=[I_m,0]$ and $E_{p1}^T=[I_p,0]$ with $I_m$ and $I_p$ being identity matrices of order $m$ and $p$ respectively, and 0 a zero matrix of appropriate dimensions. Note that the block matrix $H_{rs}(k)$ in Ref. 6 is somewhat different from that shown in Eq. (5).

## Accuracy Indicators

Due to measurement noise, nonlinearity, and computer roundoff, the block matrix $H(k)$ will usually be of full rank which does not, in general, equal the true order of the system under test. It should not be the aim to obtain a system realization which exactly reproduces the noisy sequence of data. A realization which produces a smoothed version of the sequence, and which closely represents the underlying linear dynamics of the system, is more desirable. Several accuracy indicators have been investigated for quantitatively partitioning the realized model into pure (principal) and noise (perturbational) portions so that the noise portion can be disregarded. Two principal indicators now available are the singular values of block data matrix and a parameter referred to as Modal Amplitude Coherence. The number of retained singular values determines the order of the realization, and Modal Amplitude Coherence is used to assess the resulting degree of modal purity. The remainder of this section provides the mathematical framework for establishing the relationship between these accuracy indicators and the characteristics of the noise.

### Singular Values

With the singular value decomposition applied to $H(0)$, the state space is decomposed into mutually orthogonal directions, in conjunction with the corresponding singular values which provide a measure of the gain between system input [Eqs. (12-13)].

Let the block matrix $H(0)$ be considered as the measurement of an exact block matrix $\hat{H}(0)$, additively disturbed by a noise matrix $\hat{N}$ with covariance matrix $\Phi$. If $E$ is the expected value operator, then $E(\hat{N}\hat{N}^T)=\Phi$, with the noise postulated to have

zero mean value with no loss of generality. Because $\Phi$ is a covariance matrix, it is symmetric and positive semidefinite. Thus, there exists an eigensolution of the form

$$\Phi = \phi \Lambda^2 \phi^T \tag{14}$$

where $\phi$ is an orthonormal matrix and $\Lambda^2$ is a diagonal matrix containing positive eigenvalues $\lambda_1^2 \geq \lambda_1^2 \geq \ldots \geq \lambda_N^2 \geq 0$. Introduce a new error matrix $\hat{N}_\phi$ by means of the transformation

$$\hat{N}_\phi = \phi^T \hat{N} \tag{15}$$

The covariance of the matrix $\hat{N}_\phi$ becomes

$$\Phi_\phi = E(\hat{N}_\phi \hat{N}_\phi^T) = E(\phi^T \hat{N} \hat{N}^T \phi) = \Lambda^2 \tag{16}$$

The eigenvalue problem (Eq. 14) can be interpreted as that of finding the directions of the principal axes (eigenvectors) for which the covariance matrix $\Phi$ becomes diagonal. All the eigenvectors are collected as the columns of the square matrix $\phi$. As a result, an error ellipsoid can be computed if the error covariance matrix $\Phi$ is known. The ellipsoid is aligned with the eigenvectors and has semiaxes equal to the eigenvalues $\lambda_i$. The error ellipsoid can be used as a confidence measure, because the probability that the corresponding ellipsoid for the block matrix $H(0)$ lies within the error ellipsoid can be computed.

Observe from Eq. (8) that

$$S = H(0)H^T(0) = P_N D_N^2 P_N^T \tag{17}$$

where $S$ is termed the signal power matrix. Comparison of Eqs. (14) and (17) reveals that a "signal ellipsoid" similar to the error ellipsoid can be constructed. The semiaxes of the signal ellipsoid will have lengths equal to the singular values $d_i$, while the orientation of these axes will be governed by the column vectors of the orthonormal matrix $P_N$.

The error ellipsoid is characterized by the eigenvalues $\lambda_1 \geq \lambda_2 \geq \ldots \geq \lambda_N \geq 0$, while the signal ellipsoid is characterized by the singular values $d_1 \geq d_2 \geq \ldots \geq d_N \geq 0$. The contribution of the $i$th semiaxis to the signal ellipsoid is measured by the singular value $d_i$. A similar statement applies to the error ellipsoid. Can these characteristic values be used to define a signal-to-noise ratio? The answer is affirmative. However, since the directions of the semiaxes for the signal ellipsoid are generally different from those for the error ellipsoid, a one-to-one ratio such as

$$d_i/\lambda_i \qquad (i = 1,2,\ldots,N) \tag{18}$$

is not meaningful. Let the signal-to-noise ratio for each semiaxis $d_i$ be defined as

$$S_{Ni} = d_i/\lambda_1 \qquad (i = 1,2,\ldots N) \tag{19}$$

This is the most conservative definition for the signal-to-noise ratio, since $\lambda_1$ is the largest semiaxis of the error ellipsoid.

The precision of a measurement is limited by the signal-to-noise ratio that exists in the measured data. Assume that the ratio is estimated to be $S_N$. If it is found that $d_1 \geq d_2 \geq \ldots \geq d_n \geq \lambda_1 S_N \geq d_{n+1} \geq \ldots \geq d_N \geq 0$, then the subellipsoid generated by the axes $d_i (i = 1,\ldots,n)$ satisfies this signal-to-noise ratio. Hence, the rank for the subellipsoid is $n$, indicating that the contribution of the axes $d_i (i = n+1,\ldots,N)$ to the block matrix $H(0)$ is negligible and can be ignored. Once this choice is made, the rank of $H(0)$ becomes $n$ and so does that for the state matrix $A$.

The physical interpretation is the following. In the directions of the state space where the free-decay response makes large excursion, characterized by a large component signal-to-noise ratio $S_{Ni}$, the noise cannot affect the amplitude significantly. On the other hand, in the directions where there are only very small excursions, indicated by a small $S_{Ni}$, the amplitude of the state-space response is dominated by the noise and hence should be disregarded.

If Eqs. (7) and (8) are examined as a whole the equality

$$H(0) = V_\xi W_\eta = [P_N D_N^{1/2}][D_N^{1/2} Q_n^T] \tag{20}$$

defines the controllability and observability Grammians as

$$W_\eta W_\eta^T = D_N \quad \text{and} \quad V_\xi^T V_\xi = D_N \tag{21}$$

The fact that the controllability and observability Grammians are equal and diagonal implies that the realized system $[A,B,C,]$ is as controllable as it is observable. The reduced model of order $n$ after deleting singular values $d_{n+1},\ldots,d_N$ is then considered as the robustly controllable and observable part of the realized system. An important observation from Eq. (21) is that the directions with small signal-to-noise ratio have less significant degrees of controllability and observability relative to the noise. It would be unwise to require a realization including these directions.

An approach for determining an optimum singular value cutoff, related to the above discussion, is the following. Let the matrices $P_n$ and $P_0$ denotes respectively the first $n$ and the last $N-n$ columns of the orthonormal matrix $P_N$ defined in Eq. (8). Consider the projections of the exact block matrix $H(0)$ and the noise matrix $\hat{H}(0)$ and the noise matrix $\hat{N}$ onto the base matrix $P_N$. This leads to the expression

$$E_{rr}(n) = \begin{bmatrix} P_n^T H(0) \\ 0 \end{bmatrix} - P_N^T \hat{H}(0) = \begin{bmatrix} P_n^T \hat{N} \\ -P_0^T H(0) \end{bmatrix} \tag{22}$$

The zero matrix, 0, results from the singular value truncation. Equation (22) defines the error between the approximate block matrix constructed by retaining only the singular values $d_i (i = 1,\ldots,n)$ and the exact block matrix $\hat{H}(0)$. Based on the assumption that the noise $\hat{N}$ is a zero-mean process with covariance matrix $\Phi$, the expected value of the error matrix $E_{rr}(n)$ becomes

$$E(\Xi) = E[E_{rr}(n) E_{rr}^T(n)] = \begin{bmatrix} P_n^T \Phi P_n & 0 \\ 0 & P_0^T \hat{H}(0) \hat{H}^T(0) P_0 \end{bmatrix} \tag{23}$$

Taking the trace of expression (23) yields

$$Tr(E(\Xi)) = \sum_{i=1}^{n} p_i^T \Phi p_i - \sum_{i=1}^{n} p_i^T \hat{H}(0) \hat{H}^T(0) p_i + \sum_{i=1}^{N} p_i^T \hat{H}(0) \hat{H}^T(0) p_i \tag{24}$$

where $p_i$ is the $i$th column of matrix $P_N$. Since the last term in Eq. (24) is independent of $n$, the trace becomes minimum when $n$ is chosen such that

$$p_i^T \Phi p_i < p_i^T \hat{H}(0) \hat{H}^T(0) p_i \quad (i = 1,\ldots,n) \tag{25}$$

$$p_i^T \Phi p_i \geq p_i^T \hat{H}(0) \hat{H}^T(0) p_i \quad (i = n+1,\ldots,N) \tag{26}$$

The cutoff singular value $d_i$ is thus

$$d_i^2 = p_i^T H(0) H^T(0) p_i = p_i^T [\hat{H}(0) \hat{H}^T(0) + \Phi] p_i$$

$$d_i^2 > 2 p_i^T \Phi p_i \quad (i = 1,\ldots,n) \tag{27}$$

and

$$d_i^2 \leq 2 p_i^T \Phi p_i \quad (i = n+1,\ldots,N) \tag{28}$$

If the standard deviation of each entry of the noise matrix $\hat{N}$ is a constant $\sigma$ and the noise is uncorrelated (white), the matrix $\Phi$ becomes $N\sigma^2 I$, where $I$ is an identity matrix. In this case, Eqs. (27) and (28) reduce to

$$d_i^2 > 2N\sigma^2 \quad (i=1,\ldots,n) \tag{29}$$

$$d_i^2 \leq 2N\sigma^2 \quad (i=n+1,\ldots,N) \tag{30}$$

The question arises as to why the trace of Eq. (23) is taken and what the significance is. Let an ellipsoid be constructed using the eigenvalues of the positive symmetric matrix $E(\Xi)$ in Eq. (23). The semiaxes of this ellipsoid will have lengths equal to the square roots of the eigenvalues of $E(\Xi)$. Since the sum of the eigenvalues of a matrix is equal to the trace of the matrix, minimizing the trace shown in Eq. (24) also minimizes the sum of the semiaxes of the ellipsoid. $E(\Xi)$ in Eq. (23) is interpreted as the statistically expected error between the exact state impulse response and the noisy state impulse response when projected on its main $n$-dimensional subspace. For each additional dimension allowed in the realization, the sum of the semiaxes of the $E(\Xi)$ ellipsoid will increase due to additional additive noise $p_{n+1}^T \Phi p_{n+1}$ and decrease due to additional signal $p_{n+1}^T \hat{H}(0)\hat{H}^T(0)p_{n+1}$. This opposing dependency indicates the existence of an optimum order.

Note that a different treatment for the error matrix $E_{rr}(n)$ in Eq. (22) can result in a somewhat different solution for the cutoff singular value $d_n$. If the Frobenius norm of the error matrix $E_{rr}(n)$ is minimized, for example, a result similar to but different from Eqs. (27) and (28) can be found.[11,12]

### Degree of Modal Purity

It is unlikely that the reduced block matrix formed by truncation of singular values will have the same rank as that of the true underlying system, unless the noise level is sufficiently small. Since portions of the noise are still present in the reduced block matrix, a method to assess the strength of the residual noise effects is needed.

After the truncation of singular values $d_{n+1},\ldots,d_N$, as discussed in the last sub-section, the matrix $A$ has rank $n$. Find the eigenvalue and eigenvector matrices $Z$ and $\Psi$ such that

$$\Psi^{-1} A^k \Psi = Z^k \tag{31}$$

The desired modal damping rates and damped natural frequencies are simply the real and imaginary parts of the eigenvalues, after transformation from the $z$- to the $s$-plane using the relationship

$$s = [(\ell n z) \pm 2\pi i j] / [\Delta\tau i; \qquad i = \sqrt{-1} \tag{32}$$

where $\Delta\tau$ is the data sampling interval and $j$ is an integer.

The triple $[Z, \Psi^{-1}B, C\Psi]$ is obviously a minimum-order realization.[6] The columns of $C\Psi$ are the desired mode shapes, and the rows of $\Psi^{-1}B$ are the corresponding modal participation factors (initial modal amplitudes).

When the realized system $[A,B,C,]$ is transformed from state space to modal space, it includes both the true modal space and a noise modal space. For an ideal linear system, the eigenvalues and corresponding eigenvectors in the true modal space are deterministic however the block data matrix [Eq. (5)] is formed. In contrast, all modal parameters in the noise modal space are arbitrary (that is, not deterministic). Because of this arbitrariness, the two modal spaces cannot, in general, be completely separated. With this background, the Degree of Modal Purity (DMP), of which the Modal Amplitude Coherence is a special case, is developed in the remainder of this section.

The goal is to explore the algebraic framework and then induce a formulation for the measurement of DMP. Although a square ($N \times N$) block data matrix is used, any nonsquare matrix can be treated with the same scheme and carried through naturally.

For simplicity, let the block data matrix $H(k)$ be constructed using $t_i = \tau i (i=1,2,\ldots,n_c)$ and $s_j = j (j=1,2,\ldots,n_r)$ such that

$$H(k-1) = \begin{bmatrix} Y(k), & Y(k+\tau),\ldots, & Y(k+\tau n_c) \\ Y(k+1), & Y(k+1+\tau),\ldots, & Y(k+1+\tau n_c) \\ \vdots & \vdots & \vdots \\ Y(k+n_r), & Y(k+n_r+\tau),\ldots, & Y(k+n_r+\tau n_c) \end{bmatrix} \tag{33}$$

where $\tau$ is an interger and $m\,x(n_c+1) = p\,x(n_r+1) = N$, with $m$ being the number of inputs and $p$ the number of outputs. *Let* $E_{mi}^T = [0_m,\ldots,0_m,I_m,0_m,\ldots,0_m]$, where $I_m$ is an identity matrix of order $m$ located at the $i$th block column and $0_m$ is a zero matrix of order $m$. A similar definition applies to the notation $E_{pj}^T = [0_p,\ldots,0_p,I_p,0_p,\ldots,0_p]$. Examination of Eqs. (8), (11-13), (31), and (33) yields

$$\begin{aligned} Y(\tau+1) &= E_{p1}^T H(0) E_{m2} \\ &= [E_{p1}^T P_N D_N^{1/2} \Psi]\,[\Psi^{-1} D_N^{1/2} Q_N^T E_{m2}] \\ &= [C\Psi]\,[\Psi^{-1} D_N^{1/2} Q_N^T E_{m2}] \end{aligned}$$

and

$$\begin{aligned} Y(\tau+1) &= E_{p1}^T H(\tau) E_{m1} \\ &= E_{p1}^T P_N D_N^{1/2} [D_N^{-1/2} P_N^T H(\tau) Q_N D_N^{-1/2}] D_N^{1/2} Q_N^T E_{m1} \\ &= E_{p1}^T P_N D_N^{1/2} [A^\tau + \Delta] D_N^{1/2} Q_N^T E_{m1} \\ &= [E_{p1}^T P_N D_N^{1/2} \Psi]\,[Z^\tau + \Psi^{-1}\Delta\Psi]\,[\Psi^{-1} D_N^{1/2} Q_N^T E_{m1}] \\ &= [C\Psi]\,[Z^\tau + \Psi^{-1}\Delta\Psi]\,[\Psi^{-1}B] \end{aligned} \tag{34}$$

where $\Delta$ is an error matrix due to noise. When $k=\tau$ [where $k$ is the shift used in Eq. (11)], the matrix $\Delta$ represents the error resulting from the truncation of singular values. For the noise-free case, the equation $A^\tau = D_n^{-1/2} P_n^T H(\tau) Q_n D_n^{-1/2}$ holds[6] and thus $\Delta = 0$.

The eigenvalues of $A$ are preserved whatever value the integer $\tau$ takes. Therefore, if some system modes $z_i$ are highly linear and affected little by the noise, the corresponding eigenvectors $\psi_i$ will make the following equation approximately true

$$[D^{-1/2} P_N^T H(\tau) Q_N D^{-1/2}]\,\psi_i = \psi_i z_i^\tau \tag{35}$$

for all values of $\tau$. This result leads to the condition that $\Delta\psi_i \approx 0$. It simply means that the projection of the error matrix $\Delta$ on the system eigenvector $\psi_i$ is very small.

Let $\bar{\psi}_i^T$ denote the $i$th row of the matrix inverse $\Psi^{-1}$. The condition $\Delta\psi \approx 0$ then implies that $\bar{\psi}_i^T \Delta \approx 0$. Now, observe from Eq. (34) that the following result holds for arbitrary $C$

$$Z^\tau \Psi^{-1} B - \Psi^{-1} D_n^{1/2} Q_N^T E_{m2} = \Psi^{-1} \Delta B \tag{36}$$

In terms of each individual mode, Eq. (36) becomes

$$z_i^\tau \bar{\psi}_i^T B - \bar{\psi}_i^T D_N^{1/2} Q_N^T E_{m2} = \bar{\psi}_i^T \Delta B \tag{37}$$

The smaller the elements of $\bar{\psi}_i^T \Delta B$ are, the more the mode exhibits linear, ideal behavior. All the numbers on the left side of Eq. (37) are known, and the computation of the error number is a simple operation.

If $\tau$ is replaced by $\tau j$ in Eq. (34), an equation similar to Eq. (37) can then be obtained as follows

$$z_i^{\tau j}\bar{\psi}_i^T B - \bar{\psi}_i^T D_N^{1/2} Q_N^T E_{m(j+1)} = \bar{\psi}_i^T \Delta B$$

$$\text{for} \quad i = 1,2,\ldots,n \text{ and } j = 1,2,\ldots,n_c \tag{38}$$

Based on Eqs. (37) and (38), the degree of Modal Amplitude Coherence[6] can be defined in terms of *each modal history* $\bar{\psi}_i^T D_N^{1/2} Q_N^T E_{m(j+1)}$; $(j=1,\ldots,n_c)$ and *a corresponding extrapolated modal history* $z_i^{\tau j}\bar{\psi}_i^{-T} B$. Define a column vector $q_i$ as

$$q_i^* = \bar{\psi}_i^T D_N^{1/2} Q_N^T [E_{m1}, E_{m2}, \ldots, E_{mn_c}]; \quad i = 1,2,\ldots,n \tag{39}$$

where (*) means transpose and complex conjugate. Also consider the sequence $\tilde{q}_i$, where

$$\tilde{q}_i^* = [1, z_i^{\tau}, z_i^{2\tau}, \ldots, z_i^{\tau n_c}]\bar{\psi}_i^T B; \quad i = 1,2,\ldots,n \tag{40}$$

Let $\gamma_i$ denote the Modal Amplitude Coherence which measures the degree of the $i$th modal purity, satisfying the relation

$$\gamma_j = |\tilde{q}_j^* q_j| / [(\tilde{q}_j^* \tilde{q}_j)(q_j^* q_j)]^{1/2}; \quad j = 1,2,\ldots,n \tag{41}$$

where $|\ |$ represents the absolute value. The parameter $\gamma_j$ takes only the values between 0 and 1. $\gamma_j \to 1$ as $q_j \to \tilde{q}_j$ indicates that the realized system eigenvalue $s_j$ is very close to the true value for the $j$th mode of the system. On the other hand, if $\gamma_j$ is considerably smaller than 1, the $j$th mode is considered to be a noise mode. Obviously, the parameter $\gamma_j$ quantifies the degree to which mode $j$ was excited by a specific input.

For the case where $\tau = k$ and no singular values are truncated, $\Delta = 0$, which causes the parameter $\gamma_j (j = 1,2,\ldots,n)$ to always equal 1, since there is no error vector projection on the modal base vector [see Eq. (36)]. To avoid this, the shift parameter $\tau$ is usually chosen to be larger than $k$, particularly for a square block matrix, as shown in Eq. (33). The above statments are also true for a rectangular block matrix, if the column number is less than the row number.

Based on Eq. (38), the DMP could be defined differently from the Modal Amplitude Coherence given by Eq. (41). For example, if a vector norm of Eq. (38) is taken, a different form of the equation for the parameter $\gamma_j$ can be derived.

The algebraic framework developed in this section, such as Eq. (34), can be easily generalized to cover the case of a general form of the block data matrix [Eq. (5)]. Instead of the column shift with multiplicity $\tau$ as shown in Eq. (33), a row shift can also be used to derive an equation similar to Eq. (36) in which $B$ and $E_{mi}$ are replaced by $C$ and $E_{pj}$, respectively, with slightly different matrix operations. If $\tau$ and $E_{m1}$ are replaced by $t_i$ and $E_{mi}$, respectively, Eq. (34) becomes the key algebraic formulation for any general block matrix. In practice, the block matrix of Eq. (33) and its induced formulations such as Eq. (41) are somewhat easier for computer implementation.

## Numerical Simulations

Numerous Monte Carlo simulations[9] have been conducted to study the ERA technique numerically. In this approach, a large number of data sets are generated for each desired case using the same modal parameters and noise level, but with the noise in each set consisting of a different sequence of random numbers. All data sets are then analyzed in the same manner with the identification technique. Information from each case consists of statistical measures of the results, typically the mean and standard deviation of each identified parameter.

Sample results obtained by this process for a simple four-mode system, using two different levels of additive noise, are discussed in the remainder of the paper. These cases were selected to illustrate several of the concepts discussed earlier. Each result is based on the Monte Carlo analysis of 100 data sets.

### Construction of Data Sets

Table 1 contains the parameters used in developing the simulated data sets. A four-mode, four-measurement system was arbitratily selected. For each measurement position $n$, a simulated free-response function was constructed as the summation of four exponentially weighted sinusoids plus noise as follows:

$$y_n(k) = \sum_{m=1}^{4} A_{nm} e^{-\zeta_m \Omega_m t_k} \cos(\omega_m t_k - \theta_{nm}) + w_n(k)$$

$$n = 1,2,3,4 \tag{42}$$

where $\omega_m = 2\pi f_m$; $\Omega_m = \omega_m/(1-\zeta_m^2)^{1/2}$; and $w_n(k) =$ white noise.

Observe from Table 1 that the amplitudes of the four modes decrease monotonically, going from mode 1 at 1 Hz to mode 4 at 4 Hz. This situation will cause noise to affect the higher-numbered modes to a greater degree than the lower-numbered modes. Also note that a damping value of zero was selected for all four modes. Though this level is unrealistic, it was chosen to permit the performance of the identification algorithm to be studied without accounting for a decrease in signal-to-noise ratio which occurs as a function of time in the damped case. The inclusion of this additional effect would have unnecessarily complicated the goals of the present investigation. The trends in the results to be shown will also occur when damped modes are used. Depending on the level of damping, though, the results will be somewhat noisier due to the decreasing signal-to-noise ratio with time.

The results for two different levels of added noise will be discussed. These cases are referred to as "20% noise" and "1% noise" and use white noise, which is uniformly distributed over amplitudes $\pm 0.20$ and $\pm 0.01$ units, respectively. The maximum response level of any mode is $\pm 1.0$ unit of amplitude.

Most experimental measurements have less than 20% overall noise, and many have less than 1%. However, although overall measurement noise may be low, structural dynamics data will nearly always contain contributions from modes with response amplitudes close to or below the noise floor. The effects of noise on these lower-amplitude modes is the situation addressed by the simulations. The use of uniformly distributed white noise represents the effects of analog-to-digital quantization on these low-amplitude modes. Proportionately better results can be expected for modes with larger relative amplitudes than those used in the simulations (assuming nonlinearity is not a factor).

**Table 1 Parameters used in constructing simulation data sets**

| | | Mode no. | | | |
|---|---|---|---|---|---|
| | | 1 | 2 | 3 | 4 |
| Frequency, Hz ($f$); | | 1.00 | 2.00 | 3.00 | 4.00 |
| Damping factor ($\zeta$); | | 0.00 | 0.00 | 0.00 | 0.00 |
| Amplitude ($A$): | | | | | |
| Measurement | 1 | 0.1 | 0.5 | 0.1 | 0.05 |
| | 2 | 1.0 | 0.05 | −0.1 | −0.05 |
| | 3 | −1.0 | −0.5 | 0.01 | 0.05 |
| | 4 | 1.0 | 0.5 | 0.1 | 0.005 |

Phase angle ($\theta$): All 90 deg
Noise: Uniformly distributed, white

| | | Amplitude | Std. deviation |
|---|---|---|---|
| Case 1 | 20% Noise | ±0.20 | 0.1155 |
| Case 2 | 1% Noise | ±0.01 | 0.0058 |

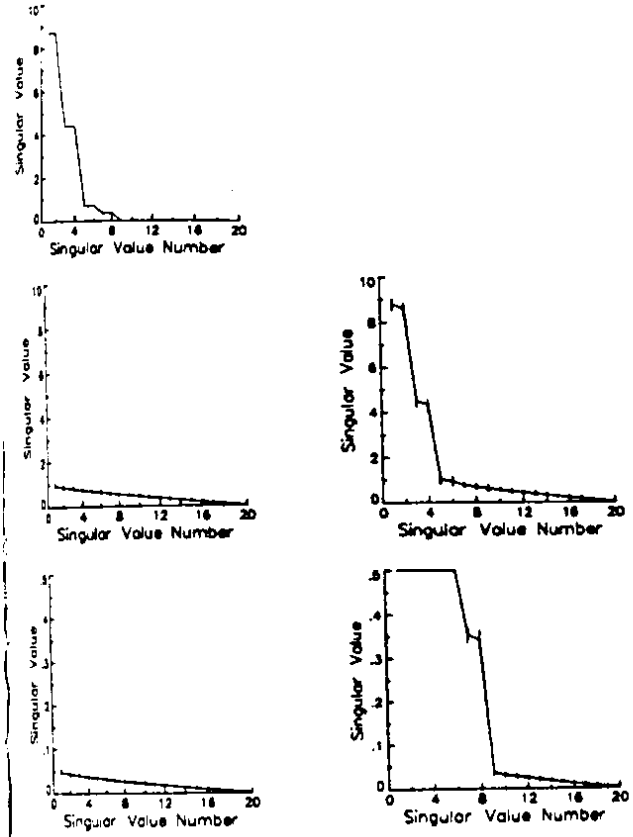


Fig. 1 Singular value spectra for simulated data sets. Vertical lines show extent of scatter in each Monte Carlo analysis.

The time histories were constructed using a sampling frequency of 10 Hz.

### Selection of ERA Analysis Parameters

All results to be shown were obtained using a square $20 \times 20$ block data matrix [Eq. (5)]. The shift parameters between block rows and between block columns were $s_j = 2j (j = 1,2,\ldots,19)$ and $t_i = 3i (i = 1,2,\ldots,19)$, respectively. A shift of one data sample ($k = 1$) was used in calculating the $A$ matrix [Eq. (11)].

### Singular Value Results

The singular value spectra obtained in this study are shown in Fig. 1. The results for the case of no added noise are presented first. It is apparent from Fig. 1a that there are exactly eight non-negligible singular values. This occurs because four modes were used in the simulation (each of which is a second-order process). Singular values 9-20 are all less than $10^{-12}$, compared with a computer precision of approximately $10^{-14}$. For all practical purposes they are zero.

Next, the results obtained using the 20% noise sequence alone are shown. The data samples in this case are the same set of random numbers that will be used to corrupt the simulated measurements for the 20% noise case, to be discussed next. One might expect the singular value spectrum for white noise to be flat, since there are no deterministic components. However, as can be seen in Fig. 1b, the computed spectrum is not flat, but varies rather linearly from an amplitude of 1.0 to approximately 0.0. This compares with an expected amplitude of 0.516, which can be calculated using the standard deviation of the noise samples (given in Table 1).

The vertical lines appearing in Figs. 1b-e show the extent of scatter among the 100 separate results obtained in each Monte Carlo analysis. The central line connects the average value for each case.

The singular value results for the 20% added noise case — using data consisting of the sum of the data used for the results in Figs. 1a and 1b — are presented next in Fig. 1c. The resulting singular-value spectrum is approximately the sum of the two previous spectra. Note in this case, though, that the four smallest singular values have become dominated by the effects of noise. This condition will cause the identification results for the lower-amplitude modes to become very noisy, as will be seen in Fig. 2. Although the presence of mode 3 will still be (barely) detected in this case, the accuracy of the parameters has been affected to a considerable degree. Mode 4 will be undetectable in this case.

An optimum singular value cutoff of 0.73 can be calculated for this case using Eqs. (29) and (30) and the known standard deviation of the noise. From Fig. 1c, this cutoff value corresponds to approximately the eighth singular value. As the results in Fig. 2 will demonstrate, reducing the order of the model to eight is indeed a good choice for this case.

A less-conservative cutoff value could be calculated by increasing the value determined above by a factor of two, since the highest singular value of the noise alone, Fig. 1b, is about twice the average value. This alternative cutoff of 1.4 corresponds to approximately the fourth singular value. As will be seen in Fig. 2, the use of a fourth-order model results in somewhat improved accuracy for the first two modes at the expense of the higher modes. Thus, a better compromise between accuracy and the number of detected modes is obtained using an eighth-order model, as suggested above.

The final two plots in Fig. 1 d and e show the results for the 1% noise case and are the counterparts of the two previous plots. The singular value spectrum of the noise alone shown in Fig. 1b, except reduced in amplitude by a factor of 20. This behavior was expected, since the same random number sequence as before was used, the only difference being in amplitude. The reduction in the magnitude of the noise from 20% to 1% has allowed all of the first eight singular values to now rise above the effects of noise. Using Eqs. (29) and (30), a singular value cutoff of 0.036 is calculated. From Fig. 1e, this value corresponds to approximately the 10th singular value. Figures 3 and 4, to be presented later, will show that this order is also an optimum choice. As before, an alternative singular value cutoff of 0.073 can be calculated by doubling the result obtained above. In this case, the alternative model order would be eight, which is the true order of the system.

### Identified Frequencies vs Order of Reduced Model

A fundamental measure of the effects of noise on the identification results is the variance (and mean value) of the natural frequency estimates. These effects are quantified in the remaining figures. Figures 2(a)-(f) show a complete set of identified frequencies for all 100 data sets in each of six different Monte Carlo analyses at 20% noise. Each of parts a-f is identical except that the number of retained singular values ("ORDER") varies. The ordinate label "Case No." refers to the data set number within each Monte Carlo analysis, and ranges from 1 to 100. Figure 3 is identical to Fig. 2, except for the 1% noise situation.

Each data point in Figs. 2 and 3 is actually a short, vertical line segment whose height is proportional to the value of Modal Amplitude Coherence.[6] The line segments are located horizontally in the plots at the corresponding identified frequencies. If the Modal Amplitude Coherence is 100% (its maximum value), the height of the line segment equals the distance between the tic marks on the vertical axis. Smaller values of coherence result in dots and shorter-length dashes. The strongest identification results are thus indicated by an unbroken vertical line extending from case 1 to case 100, and located horizontally at the correct natural frequency. Only eigenvalues with a Modal Amplitude Coherence of at least 10% are shown. All those with smaller values are considered to be noise modes, or system modes dominated by noise.

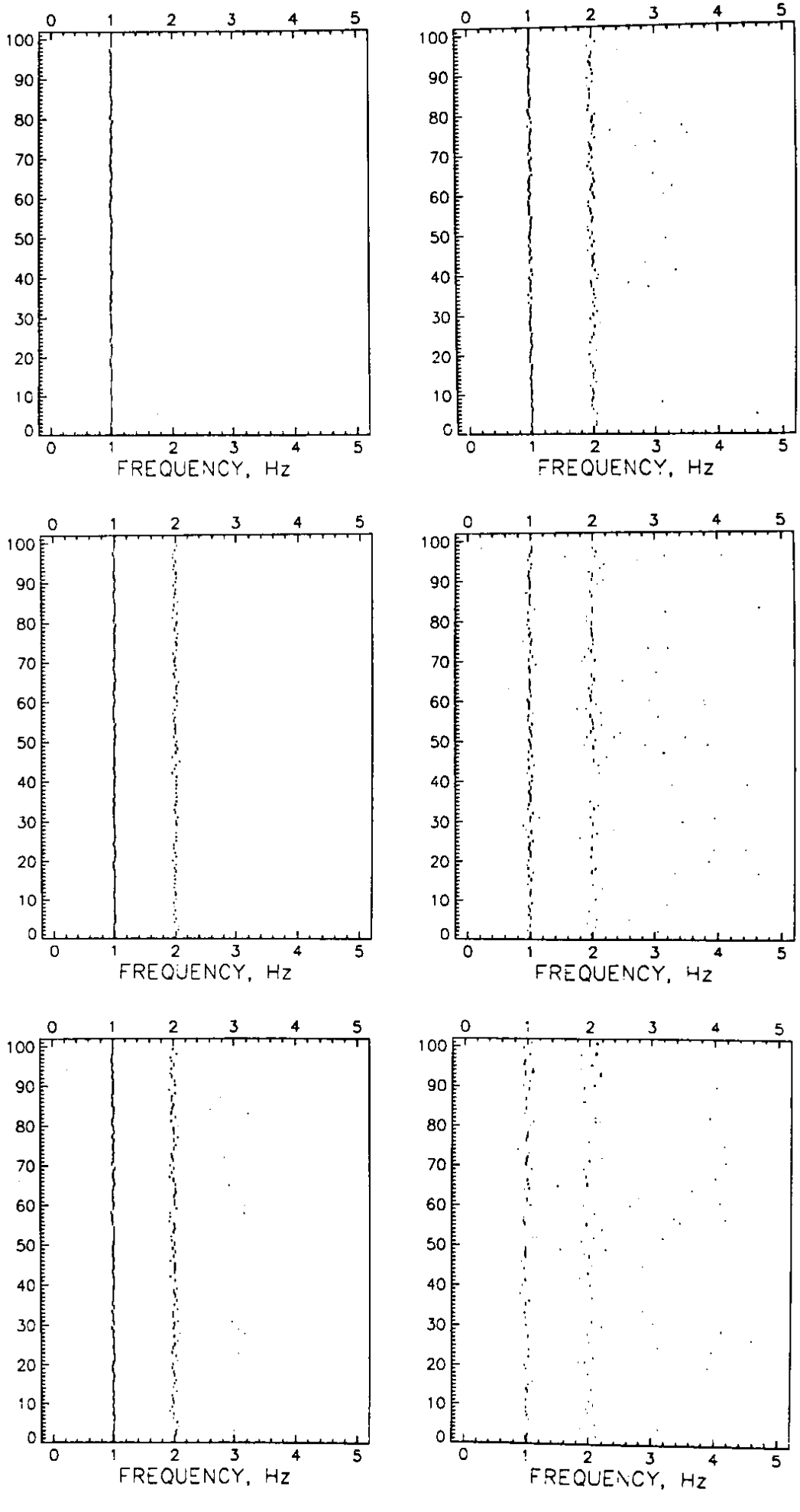


**Fig. 2 20%-noise results at various values of ORDER (the number of retained singular values). All identified frequencies with Mod Amplitude Coherence of at least 10% are shown.**

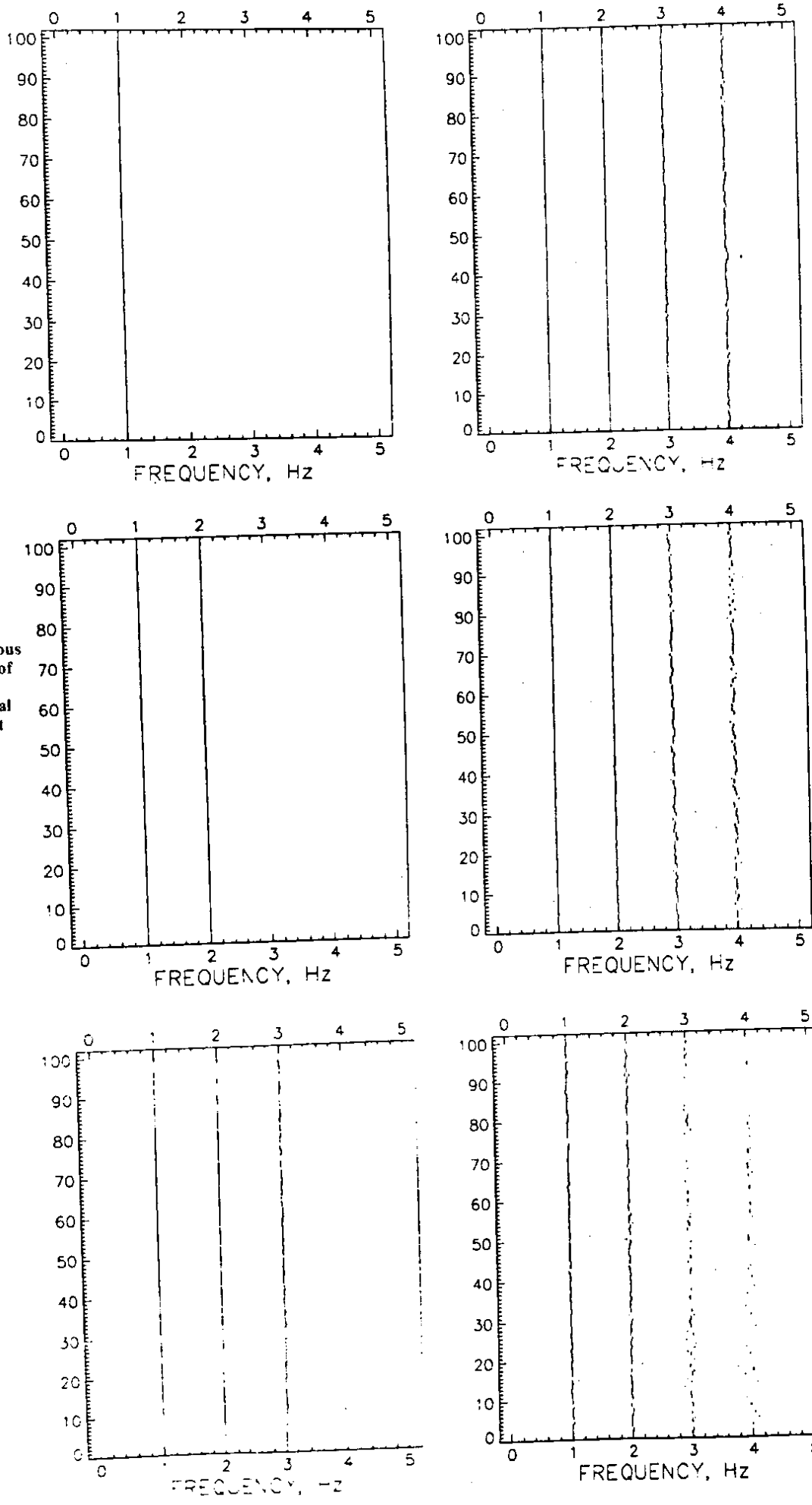


Fig. 3 1%-noise results at various values of ORDER (the number of retained singular values). All identified frequencies with Modal Amplitude Coherence of at least 10% are shown.

Inspection of Figs. 2a-f shows that only the first mode (at 1 Hz) is identified when ORDER equals 2, and that only the first two modes (1 and 2 Hz) are significant at any value of ORDER up to the maximum of 20. The complete disapperance of all modes except the first in Fig. 2a is explained by the fact that only one mode can be identified with a second-order solution, and that the first has the highest signal-to-noise ratio among those used in the simulation. The difficulty in identifying modes 3 and 4 in this case correlates with the results shown earlier in Fig. 1c, in which the four smallest singular values are dominated by noise. As already discussed, the use of ORDER = 8, a value which can be calculated using Eqs. (29) and (30) and the standard deviation of the noise, is a good compromise between maintaining the accuracy of modes 1 and 2 while permitting the detection of mode 3.

The same trends in the effects of noise on the identified frequencies are observed in Fig. 3, which shows corresponding results for 1% noise. Notice first that when ORDER is lowered below the value of eight (the true order of the system), the lowest-amplitude mode disappears first. For example, in Fig. 3c, note that only modes 1, 2, and 3 are present in the results. Since a sixth-order solution was used, a maximum of three modes can be found. Mode 4, which had the lowest amplitude among the four modes, is the one rejected automatically in the model reduction process (via singular value truncation). A similar effect is observed in Figs. 3a and 3b.

A second item to note from Fig. 3 is that the identification scatter increases for all modes as ORDER increases above the value of eight. Thus, eight is certainly a good choice for the order of the reduced model. As discussed earlier, a value of 10 was calculated for the optimum order using Eqs. (29) and (30), and a value of eight using the alternative choice. The value of eight is considered less conservative since inadvertently choosing too small an order is typically worse from an overall accuracy standpoint than choosing too large an order.

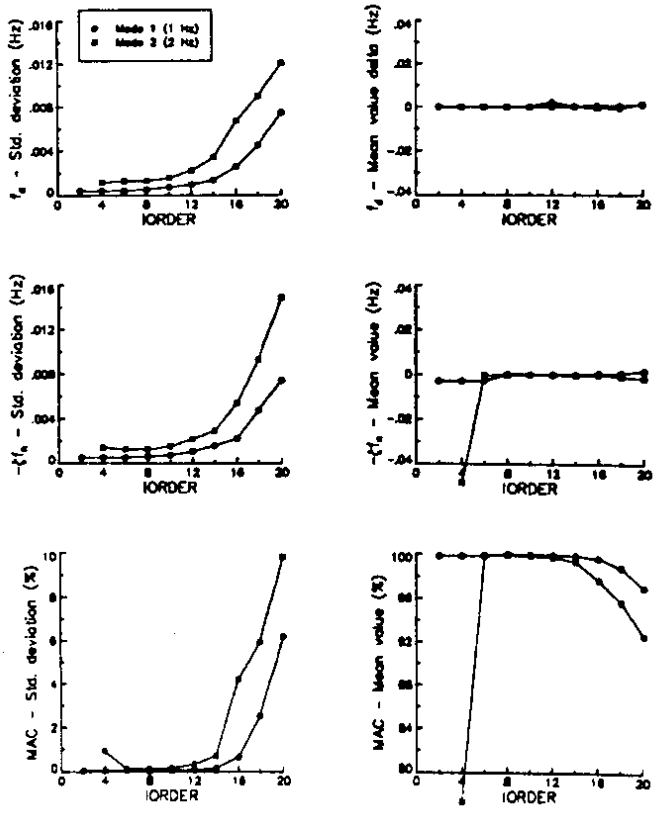


**Fig. 4 1%-noise identification statistics for modes 1 and 2 vs ORDER (the number of retained singular values).**

### Eigenvalues and Modal Amplitude Coherence

The final figure, Fig. 4, presents the results of standard deviation and mean value calculations performed for the 1%-noise Monte Carlo analyses. Frequency, damping, and Modal Amplitude Coherence statistics for modes 1 and 2 are shown. Trends in the results for modes 3 and 4 are similar to those for modes 1 and 2.

Figures 4a-d show the results for the identified eigenvalues (whose real part is the damping and whose imaginary part is the frequency) as a function of ORDER, the order of the reduced model. As already seen in Fig. 3, the standard deviation in the identified eigenvalues increases as ORDER rises above a value of eight or ten. Below this point, the standard deviation is approximately constant, though a slight upward trend is detected in Fig. 4c for mode 2. The important thing to note from these results is that the scatter in the identified eigenvalues decreases by about an order of magnitude as ORDER is lowered from 20 to 8. Also, in addition to being about ten times more accurate, the eighth-order model, requiring only an eighth-order eigensolution, entails many fewer calculations than the 20th-order model, which requires a 20th-order eigensolution. The truncation of those singular values attributed to the noise undoubtedly acted as an effective noise filter. The accuracy advantages over identification methods which do not permit order reduction independent of the size of the block data matrix (Ref. 4, p. 186) are clear.

The eigenvalue mean value results, presented in Figs. 4b and 4d, show essentially no bias for model orders of eight and larger. When fewer than eight singular values are retained, however, significant damping biases are observed. In particular, the bias is very large for mode 2 when the order is reduced to four.

The final two plots in Fig. 4 show the corresponding results for Modal Amplitude Coherence. The intent of this indicator is to provide an automatic means for assessing the degree to which each eigenvalue retained in the reduced model is influenced by noise. Larger values of the indicator (up to 100%) correspond to purer modal responses. The Modal Amplitude Coherence results in Figs. 4e and 4f correlate well with the earlier observation that optimum singular-value truncation can significantly improve the accuracy of the final model. Considerable reductions in the standard deviation and increases in the mean value of Modal Amplitude Coherence occur as the order of the model is reduced from 20 to 8.

## Concluding Remarks

The error characteristics due to noise of the Eigensystem Realization Algorithm have been studied analytically and numerically. Contributions of this work include a method for computing an optimum singular value cutoff knowing the covariance structure of the noise, and an explicit description of the effects of noise on the accuracy indicator referred to as Modal Amplitude Coherence. The analyses were substantiated by numerical simulations using the Monte Carlo technique. The numerical results demonstrated that an order of magnitude improvement in identification accuracy is possible using model reduction via optimum singular-value truncation.

## References

[1]Graupe, D., *Identification of Systems,* R.E. Krieger Publishing Co., Malabar, FL, 1976.

[2]Goodwin, G.C. and Payne, R.L., *Dynamic System Identification: Experiment Design and Data Analysis,* Academic Press, New York, 1977.

[3]Ljung, L. and Soderstrom, T., *Theory and Practice of Recursive Identifiation,* MIT Press, Cambridge, MA, 1983.

[4]Ewins, D.J., *Modal Testing: Theory and Practice,* John Wiley and Sons, Inc., New York, 1984.

[5]Ho, B.L. and Kalman, R.E., "Effective Construction of Linear State-Variable Models From Input/Output Data," *3rd Annual Aller-*

*ton Conference on Circuit and System Theory*, 1965, pp. 449-459; also *Regelungstechnik*, Vol. 14, 1966, pp. 545-548.

[6]Juang, J.-N. and Pappa, R.S., "An Eigensystem Realization Algorithm (ERA) for Modal Parameter Identification and Model Reduction," *Journal of Guidance, Control and Dynamics*, Vol. 8, Sept.-Oct. 1985, pp. 620-627.

[7]Pappa, R.S. and Juang, J.N., "Galileo Spacecraft Modal Identification Using an Eigensystem Realization Algorithm," *Journal of the Astronautical Sciences*, Vol. 33, Jan.-Mar. 1985, pp. 15-33.

[8]Brumfield, M.L., Pappa, R.S., Miller, J.B., and Adams, R.R., "Orbital Dynamics of the OAST-1 Solar Array Using Video Measurements," AIAA Paper 85-0758, April 1985.

[9]Rubinstein, R.Y., *Simulation and the Monte Carlo Method*, John Wiley & Sons, Inc., Somerset, NJ, 1981.

[10]Klema, V.C. and Laub, A.J., "The Singular Value Decomposition: Its Computation and Some Applications," *IEEE Transactions on Automatic Control*, Vol. AC-25, April 1980, pp. 164-176.

[11]Staar, J., Vandewalle, J., and Wemans, M., "Realization of Truncated Impulse Response Sequences with Prescribed Uncertainty," *Proceedings of the IFAC Control Science and Technology (8th Triennial World Congress)*, Kyoto, Japan, Aug. 1981, pp. 7-12.

[12]Staar, J., Vandewalle, J., and Wemans, M., "A General Class of Numerically Reliable Algorithms for the Realization of Truncated Impulse Responses," *Proceedings of the IFAC Control Science and Technology (8th Triennial World Congress)*, Kyoto, Japan, Aug. 1981, pp. 13-19.